Experimental Study on Liquid Sloshing Characteristics in a Propellant Tank with Perforated Damping Structure on a Satellite

Zhen Qu
bejing institue of control engineering
Yong Li (li-y95@tsinghua.org.cn)
bejing institue of control engineering
Jintao Liu
bejing institue of control engineering
Kun Cai
bejing institue of control engineering
Jun Long
bejing institue of control engineering
Can Yao
bejing institue of control engineering

Research Article

Keywords: Satellite propellant tank, liquid sloshing test, equivalent pendulum model, sloshing force and moment, propellant management device (PMD)

Posted Date: February 22nd, 2023

DOI: https://doi.org/10.21203/rs.3.rs-2576419/v1

Abstract

The liquid in the satellite propellant tank is inevitably sloshing due to the vibration excitation of the rocket body. During the process of launch and satellite orbit change, the vibration excitation will be transmitted to the propellant tank. The resulting sloshing of liquid in the tank will generate additional sloshing force and moment applied on the satellite, which will have a serious impact on the satellite's attitude. In this paper, the sloshing performance of liquid in the large capacity propellant tank on the satellite is tested. The liquid sloshing tests were carried out on upper and lower tanks with a porous damping structure under different filling ratios, respectively. The mechanics data was collected by the sensor and analyzed using the classic pendulum model. Based on the test data and classic theory, the sloshing frequency, sloshing quality and sloshing damping parameters of upper and lower tanks were computed and compared. The results showed that the sloshing performance of the propellant tank was significantly affected by the internal damping structure. The research results of sloshing provide reference and support for the design and optimization of satellite attitude control.

1. Introduction

Liquid sloshing is a detrimental interfering side effect for fuel storage in engineering applications, especially in the spacecraft propulsion system. Sloshing in fuel storage tanks of spacecraft usually leads to undesired sloshing forces and moments, which must be counterbalanced by the altitude control system (Vergalla 2010, Bearman 1985). Therefore, accurate prediction of such nonlinear loads on the ground is critically important for spacecraft attitude control in operation (Nayak 2016). Combining experimental data with theoretical analysis is an effective method to study the liquid sloshing force and movement of the satellite tank (Panigrahy 2009, Maleki 2008, Yan G 2009).

NASA has been interested in fluid sloshing dynamic behaviors in aerospace missions since the 1950s to develop the Apollo program (Molin 2013). At the time the Navier-Stokes equations (Graham 1952) could not be numerically solved, thus scientists and engineers had to rely on analog methods, tests, and resulting correlations. In the 1980s and 1990s, with the emergence of powerful computers, computational fluid dynamics (CFD) was used to simulate and predict slosh with little experimental data validation (Moiseev 1964). However, the results from CFD programs require extensive experimental validation, especially several mishaps have caused the programs to be questioned over the last few years (Moiseev 1966). Therefore, further experimental confirmation is imminent and the research based on liquid sloshing tests have been favored by more and more scholars (Huang 1993, Shabana 1991).

In the experimental literature, the issue of fluid structural interaction coupling be-tween an interior item and sloshing in the container has been addressed in a variety of ways. In particular, the interior item has three different structure forms involving the typical block-type (Bearman 1985, Nayak 2016), blade-type (Panigrahy 2009, Maleki 2008) and perforated plane type (Yan 2009, Molin 2013). For the block-type structure, Bearman has investigated the flow around the interior cylinder structure under harmonically fluctuating flow (Bearman 1985). Besides, the effect of the submerged block on the nonlinear sloshing

was systematically studied by Nayak and Biswal subjected to horizontal earthquake motions (Nayak 2016). For the blade-type baffles of varying dimensions and orientations in the tank, Panigrahy focused on the pressure distributions at different locations and three-dimensional effects on liquid sloshing (Panigraghy 2009). Concerning horizontal ring and vertical blade-type baffles (Maleki 2008), an estimation of the liquid sloshing damping ratio in baffled tanks has been developed and the results have been validated by a series of experiments. The non-linear sloshing in partially filled tanks with perforated and orifice plate-type baffles was explored by Yan (Yan 2009). In addition, Molin has performed liquid sloshing experiments in a tank with vertical screens, which is subjected to forced harmonic horizontal and rolling motions(Molin 2013). However, these experimental studies did not involve the conical perforated plate structure in the real tank structure.

The paper aims to study liquid sloshing characteristics in a large-capacity propellant tank with a conical perforated type propellant management device (PMD). A set of a special frame structure for suspending the tank was designed. The sloshing characteristics and damping characteristics of the liquid in the satellite propellant tank will directly affect the attitude control of the satellite in orbit. Therefore, in this paper, the method of the sloshing test is used to simulate the sloshing force and moment generated by the satellite during orbit change. The sloshing forces and moments are obtained by the mechanical sensor fixed on the tank, which is redesigned for fitting the tank structure. The free attenuation sloshing and forced sloshing on the first-order resonance frequency are tested using full and half-layer (upper and lower half) tank respectively.

2. Experimental Tank Structure

The satellite storage tank model used in the sloshing test in this paper is shown in Fig. 1. The structure of the tank consists of four parts, including the upper tank canopy, propellant management device (PMD), connecting ring and lower tank canopy. The tank shell is composed of a plexiglass casing and an aluminum alloy frame.

The whole cabin without PMD is hoisted along the Z direction and shaken along the X direction for the test. The Z-axis direction is shown by the red dashed arrow in Fig. 1(a). The plane where the X and Y directions are located is perpendicular to the Z axis. Af-terward, three-direction liquid sloshing tests were performed on the upper tank (Fig. 2) and the lower tank (Fig. 3) of the tank divided by the mid-bottom. In this paper, the ZX vi-bration is defined as that the Z-axis of the tank is upward, and the vibration is in the X-axis direction. The XZ direction and the XY direction are also defined in the same way.

The propellant management device (PMD) of the tank consists of a middle bottom and an anti-slosh cone with mesh holes. The test tank is divided into two parts: the upper tank and the lower tank by the middle bottom. The test liquid between the upper and lower tanks can only be circulated through the screen on the middle bottom, and there is no liquid leakage between the middle bottom and the

connecting ring. The existence of the anti-slosh cone structure will directly affect the liquid sloshing damping in the tank.

3. Test Equipment And Method

3.1. Suspension test device

The test device for the liquid sloshing test is shown in Fig. 5. The tank was hoisted by the suspension system for the liquid sloshing test. The suspension system includes a suspension support frame, suspension wire rope and tank cage. The initial excitation of liquid sloshing comes from the vibration table, which acts on the suspended tank to pro-vide a certain frequency of displacement excitation.

Three parameters need to be measured during the test: the sloshing displacement of the test tank, and the forces and moments generated by the sloshing. The forces and moments here include the resultant forces produced by both the sloshing mass and the resting mass. The forces and moments here include the resultant forces produced by both the sloshing mass and the rest mass. The measuring device mainly includes a laser dis-placement sensor, "П" type force sensor and a load cell. Among them, the laser displacement sensor is used to measure the vibration displacement, which is installed on the frame beam with a measuring range of ± 20mm. Forces and moments are measured using a "П" type sensor, which is specially designed shown in Fig. 6. The load cell is mainly used for the determination of the filling ratio in the tank.

3.2. Test method

The test first carried out the pre-experiment of the whole tank without the middle bottom. The test liquid is water, which is mainly used to verify the equivalent mechanical model and the test system. The suspension method is shown in Fig. 5. The formal test consists of two states: upper tank with middle bottom state and lower tank with middle bottom state, both using 32% glycerin/water mixture (1.08g/cm3) as the test liquid. The specific test status is shown in Table 1.

Table 1
Test situation of liquid sloshing.

Tank structure	**Whole tank without PMD**	**Upper tank with middle bottom**			**Lower tank with middle bottom**		
Test liquid	Water	32% glycerin/water mixture					
Suspension direction	Vertical		Horizontal				Vertical
Sloshing direction	ZX		XZ	XY	XZ	XY	ZX
Liquid filling ratio	0.15, 0.35, 0.50, 0.64, 0.80	0.35, 0.40, 0.45, 0.50, 0.55, 0.60, 0.64, 0.73, 0.76, 0.80, 0.85, 0.89, 0.95	0.64, 0.80		0.05, 0.10, 0.15, 0.20, 0.25		
Test method	Free attenuation sloshing and forced sloshing						

During the free attenuation slosh test, the vibration frequency needs to be adjusted to reach a resonance state of the liquid in the tank. After the vibration amplitude reaches a certain range, the frame is separated from the vibration table. The time history data of the sloshing force were recorded by the sensor. The sloshing damping coefficient was calcu-lated based on the recorded data.

The forced sloshing test uses constant displacement excitation. After the sloshing is stable, the time history of the sloshing displacement, force and moment of the tank is rec-orded. The forced sloshing test was stopped after recording 50 vibration cycles. The mag-nitude, phase and frequency of displacements, forces and moments are calculated from the recorded time history data, and frequency response function values are estimated. Af-ter changing the excitation frequency, the recording shall be repeated until the test of all frequency points is completed. The test frequency should cover 0.5 to 2 times the first-order sloshing frequency.

4. Dynamic Analysis Of Liquid Sloshing In The Tank

4.1. Equivalent mechanical model

The sloshing problem of the liquid in the tank is mathematically equivalent to the vibration problem of the oscillators (Moiseev 1964, 1966). Therefore, the liquid sloshing problem can be equivalent to a set of spring-mass-damper structures coupled to the tank. For the tank with an anti-slosh device, the device will introduce nonlinear damping to the system, resulting in no theoretical solution to the sloshing problem or a large theoretical solution error. At this time, the equivalent mechanical model is still applicable, but the model parameters can only be obtained through the sloshing test, and the theoretical solution cannot be obtained. The motion equation of the equivalent theoretical model can be obtained as follows,

$$m_i \ddot{U}_{ri} + c_i \dot{U}_{ri} + m_i \frac{g_z}{L_i} U_{ri} = -m_i \ddot{U}$$

1

m_i, c_i and L_i represent the sloshing mass, equivalent viscous damping coefficient and equivalent pendulum length, respectively; U is the sloshing displacement of the tank; U_{ri} is the displacement of the i-th order sloshing mass relative to the tank. g_z stands for gravitational acceleration. The dynamic equation of the i-th order sloshing can be obtained as follows. In addition, the sloshing force and moment can also be deduced.

$$\ddot{U}_{ri} + 2\xi_i \omega_i \dot{U}_{ri} + \omega_i^2 U_{ri} = -\ddot{U}$$

2

$$F = (m_T + m_0)\ddot{U} + \sum_{i=1}^{n} m_i (\ddot{U}_{ri} + \ddot{U})$$

3

$$M = (m_T h_T + m_0 h_0)\ddot{U} + \sum_{i=1}^{n} m_i h_i (\ddot{U}_{ri} + \ddot{U})$$

4

m_T is the mass of the empty tank; h_i represents the pendulum suspension point height of the i-th liquid sloshing; h_T is the height of the liquid centroid; m_0 and h_0 are the rest mass and centroid height of the solidified part of the liquid respectively. F and M in equations (3) and (4) represent sloshing force and moment. ω_i and ξ_i are defined as the natural frequency and damping ratio of the i-th order sloshing.

4.2. Liquid free attenuation sloshing

For the sloshing attenuation test, the sloshing is dominated by the first order, and the time history of the sloshing force is the damping oscillation curve as follows (Moiseev 1964),

$$F(t) = F_0 e^{-\omega \xi t} \cos(\omega t + \phi)$$

5

Here, ω and ξ are defined as the natural frequency and damping ratio. When dF/dt equals 0, the equations (6) and (7) can be obtained.

$$\omega t_n + \phi = n\pi - \tan^{-1}\xi$$

6

$$t_n = \frac{n\pi - \phi - \tan^{-1}\xi}{\omega}$$

7

t_n is the time corresponding to the peak and valley points of $F(t)$ in Eq. (5). Substituting t_n into Eq. (5) yields Eq. (8).

$$F_n = F_0 e^{-\omega\xi t_n}\cos(n\pi - \tan^{-1}\xi) = (-1)^n \cos(\tan^{-1}\xi) F_0 e^{-\omega\xi t_n} = \frac{(-1)^n F_0}{\sqrt{1+\xi^2}} e^{-\omega\xi t_n}$$

8

F_n is the peak and valley value of the sloshing force. In this paper, the difference between the peak and valley values (amplitude difference) is used to find the curve parameters. The F_n in the test can be obtained through the sensor. According to this parameter, the damping ratio ξ can be derived inversely.

4.3. Liquid forced sloshing

For forced sloshing, the horizontal displacement of the tank can be set as follows,

$$U = U_0 e^{j\omega t}$$

9

Substitute Eq. (9) into equations (3) and (4) and the transfer function can be obtained as follows,

$$H_F(\omega) = \frac{F(\omega)}{-\omega^2 U(\omega)} = m + \sum_{i=1}^{n} m_i \frac{\omega^2}{\omega_i^2 - \omega^2 + j2\xi_i\omega_i\omega}$$

10

$$H_M(\omega) = \frac{M(\omega)}{-\omega^2 U(\omega)} = mh + \sum_{i=1}^{n} m_i \frac{h_i\omega^2}{\omega_i^2 - \omega^2 + j2\xi_i\omega_i\omega}$$

11

When the first-order sloshing is dominant, according to the measured results of $F(\omega)$, $M(\omega)$ and $U(\omega)$, the total weight m of the tank, the sloshing mass m_1 sloshing frequency ω_1, suspension point height h_1 and damping ratio ξ_1 can be obtained by using the curve fitting method. For the pendulum model of Christiaan Huygens, the pendulum length L_1 is not an independent parameter and can be represented by ω_1 and g_z.

$$L_1 = \frac{g_z}{\omega_1^2}$$

12

The pendulum length can be used to replace the sloshing frequency, and the position of the sloshing mass centroid is presented in Eq. (12).

$$h_1 - L_1 = \frac{1}{N}\sum_{k=1}^{N}\frac{M_k}{F_k} - \frac{g_z}{\omega_1^2}$$

13

In this paper, 3 times sloshing frequency is used for sampling. When the sampling frequency is higher, the sampling data is filtered, so that the sampling rate of the filtered data is approximately 3 times the sloshing frequency (Mi-an 2013).

5. Results

Before each test, the temperature of the 32% glycerol/water mixture and the viscosity corresponding to this temperature were measured. According to the actual measurement results of the relationship between the temperature and viscosity of the mixture, a trend curve is fitted as Eq. (14).

$$y = -0.0696x + 3.9714$$

14

y represents the viscosity of the mixture and x represents the temperature. During the test, the liquid temperature range is 2°C ~ 26°C, and the liquid viscosity range is from $2\times10^{-6}m^2/s$ to $4.3\times10^{-6}m^2/s$.

The results analyzed in this chapter are obtained by substituting the test data into the classical formula in Chap. 4. The test data including the sloshing force and moment are from "Π" type force and torque sensors introduced in Chap. 3.1.

5.1. Test results of the whole tank without middle bottom

According to the results of the liquid sloshing test of the whole tank without an intermediate bottom, the equivalent mechanical model is used to analyze the forces and moments collected in the test. The equivalent mechanical model results of the test data and the numerical simulation results are compared and analyzed. In addition, the sloshing mass is compared and analyzed.

The liquid sloshing test of the whole tank without the middle bottom adopts the five liquid filling ratios shown in Table 1. The filling ratio is defined as the ratio of the liquid volume in the tank to the total volume of the tank. Since the first-order liquid sloshing frequency and sloshing mass of the liquid sloshing in the liquid-filled tank play a leading role relative to the higher order (above the second-order)

[22], the sloshing mass of the experiments and simulations mentioned in this paper is the equivalent mass of the first-order liquid sloshing. With the increase of the liquid filling ratio, the liquid sloshing frequency and the sloshing mass show an increasing trend with the increase of the liquid filling ratio, which is consistent with the reference [23]. This consistency proves the correctness of the theoretical model designated in this paper.

5.2. Test results of the upper tank with middle bottom

The 32% glycerin/water mixture was used in the upper tank sloshing test, and three different tank sloshing directions (ZX, XZ, XY) were used for the sloshing test. Thirteen groups of tanks with different filling ratios were shaken in the ZX direction. In XZ and XY directions, sloshing tests were carried out on two groups of tanks with different filling ratios. The sloshing frequency results of the ZX direction test (Fig. 7) are shown in Fig. 8.

Since the PMD used in the test contains a middle bottom and an immersed anti-sloshing cone, it can be seen from Fig. 8 that the first-order natural frequency of the liquid in the immersed anti-slosh cone area is lower than the frequency of the whole tank without middle bottom. When the liquid filling ratio is 0.4, there is no opening on the anti-sloshing cone below the liquid level. The anti-slosh cone acts like reducing the diameter of the tank, resulting in a significant increase in the liquid frequency compared to the 0.35 filling ratio. When the liquid filling ratio is 0.45, the sloshing liquid in the tank begins to pass through the round hole of the anti-sloshing cone, and the liquid sloshing damping increases, which in turn leads to a decrease in the liquid sloshing frequency.

At a filling ratio of 0.45 to 0.85, the liquid level is located in the opening area of the anti-sloshing cone, and the liquid can freely pass through the opening of the PMD anti-sloshing cone. When the filling ratio is above 0.85, the liquid level is higher than the top of the anti-slosh cone. In general, when the liquid filling ratio is greater than 0.45, the liquid sloshing frequency shows an upward trend similar to the results of the whole tank sloshing test. Due to the existence of the anti-sloshing cone, the sloshing frequency of the liquid with the intermediate bottom is lower than that of the whole tank without the intermediate bottom under the same filling ratio.

The test results of the sloshing mass are shown in Fig. 9. With the increase of the liquid filling ratio, the sloshing quality of the liquid in the tank showed a trend of first rising and then falling. When the filling ratio is 0.76, the sloshing mass reaches the maximum value.

It can be seen from the above analysis that the sloshing mass and sloshing frequency of the liquid in the tank show different trends with the increase of the filling ratio. When the filling ratio is constant, the sloshing frequency in the three test directions (ZX, XZ and XY) shows a certain variation pattern, as shown in Figs. 10–12.

As shown in Fig. 10, the sloshing frequencies of the upper tank along the ZX direction (Fig. 2(a)) and the XY direction (Fig. 2(c)) at the same filling ratio are the same, but both are lower than the sloshing frequency along the XZ direction (Fig. 2(b)). From the comparison of sloshing mass and average damping shown in Figs. 11 and 12, it can be seen that under the same filling ratio, the largest sloshing mass is along the ZX direction, and the sloshing damping corresponding to this direction is the largest;

The minimum sloshing mass is in the XZ direction. In conclusion, when the tank is in the upward orientation of the z-axis, the average damping of liquid sloshing is the largest, and the damping effect of the anti-sloshing cone inside the tank is the best, But the sloshing mass in the z-axis is higher than the sloshing mass in the x-axis.

5.3. Sloshing test results of the lower the tank

The sloshing test of the lower tank has been completed in three directions of ZX, XZ and XY, and each direction has five filling ratios. To compare and analyze the test results in the three directions, the sloshing frequency, sloshing damping, sloshing mass and pendulum height with the liquid filling ratio are plotted as shown in Figs. 13–16.

In Fig. 13(b), the liquid sloshing damping causes the liquid to oscillate at its natural frequency in free-damped sloshing until it stops. In Fig. 13(a), the sloshing frequency is measured by the free-damping sloshing test of the liquid in the tank, which is the natural sloshing characteristic of the liquid in the tank. Among the sloshing frequencies in the three directions, the frequencies showed an upward trend with the increase of the filling ratio. The sloshing frequency in the XZ direction is significantly higher than that in the XZ and XY directions, and the lowest sloshing frequency is along the ZX direction where the tank is placed horizontally. In addition, the sloshing damping in the XZ direction is opposite to the decreasing trend in the other two directions. Figure 14 shows the sloshing test state in the XZ direction, and the result of sloshing damping in the XZ direction shown in Fig. 13(b) increases with the increase of the filling ratio.

To further analyze the experimental results in Fig. 13, the variation trend of sloshing mass and swing point height in three sloshing directions with liquid filling ratio was plotted, as shown in Fig. 15 and Fig. 16. The maximum height of the swing point in Fig. 16 has the same meaning as h_1 in Eq. (12). The sloshing frequency in the XZ direction is the highest, but the increasing trend of the sloshing mass is not obvious, and the sloshing mass is lower than that in the ZX and XY directions under most liquid filling ratio conditions. In contrast, the maximum height of the swing point increases significantly with the increase of the filling ratio. The sloshing frequency of the liquid is essentially determined by the inherent properties of the liquid in the tank. The maximum height of the swing point is positively related to the stiffness of the equivalent mechanical model. According to the basic theory of vibration mechanics [24], the experimental results in Fig. 13(a) that the sloshing frequency in the XZ direction is significantly higher than that in the other two directions can be explained.

5.4. Comparative analysis of test results

In the ZX sloshing direction, by comparing Fig. 8 and Fig. 13(a), the liquid sloshing frequencies of the upper and lower tanks show an upward trend with the increase of the liquid filling ratio. Since the upper tank PMD will change the liquid sloshing damping, the increase of the sloshing frequency in Fig. 8 is not a linear relationship as shown in Fig. 13(a). The sloshing frequency fluctuates when the liquid fill ratio is from 0.35 to 0.5. Similarly, the trend of the sloshing mass in the ZX direction of the upper tank with the filling ratio in Fig. 9 is also significantly different from that of the lower tank in Fig. 15. The sloshing mass of the upper tank first rises and then decreases with the increase of the liquid filling ratio, and the

sloshing mass reaches the maximum value when the liquid filling ratio is 0.76. The sloshing mass of the lower tank has no obvious peak value under the condition of a low filling ratio, and shows a linear upward trend.

In the XZ sloshing direction, by comparing Fig. 10 and Fig. 13(a), it can be seen that under the condition of a constant liquid filling ratio, the liquid sloshing frequency in the upper and lower tank is higher than that in the ZX and XY directions. On the contrary, by comparing Fig. 11 and Fig. 15, the sloshing mass in the XZ direction is the minimum value of the test results in the three directions under the condition of a constant filling ratio (0.64 and 0.8); The sloshing mass in the XZ direction of the lower tank is also the minimum value in the three directions when the filling ratio is less than 0.2, and there is a slight upward trend with the increase of the filling ratio. By comparing the sloshing damping in Fig. 12 and Fig. 13(b), the sloshing damping in the upper tank is obviously lower than that in the ZX direction. However, the sloshing damping of the lower tank is significantly higher than the ZX direction when the filling ratio is greater than 0.1, and the sloshing damping has an obvious upward trend with the increase of the filling ratio.

6. Conclusions

A large amount of experimental data and sloshing parameters obtained through the sloshing test in this paper can accurately describe and analyze the sloshing characteristics of the liquid in the large-capacity propellant storage tank. At the same time, the experimental research results can provide important reference and data support for the orbit control and attitude optimization of launch vehicles and spacecraft. Through the analysis of the liquid sloshing test data in this paper, the following conclusions can be drawn:

The experimental results of the whole tank without the middle bottom are consistent with the theoretical results, which verifies the reliability of the experimental system and the correctness of the theoretical model.

The sloshing frequency of the tank with PMD is obviously affected by the internal structure of the tank, and it shows a non-monotonic trend with the filling ratio. The liquid sloshing frequency can range from 0.5 to 1.1 Hz.

For the tank without PMD, the sloshing mass, sloshing frequency, and the height of the swing point are closely related to the sloshing direction under the same liquid filling ratio. The sloshing parameters are an important reference factor for the design of the tank.

The ground test in this paper adopts a real propellant tank structure, and the sloshing direction and liquid filling ratio of the test conditions are also obtained according to the real satellite on-orbit conditions. According to the analyzed results, the anti-sway structure of the tank can be optimized on the one hand, on the other hand, the attitude adjustment procedure of the satellite in orbit can be optimized to make the orbit change of the satellite more stable.

Declarations

Acknowledgements

This work was supported by National Natural Science Foundation of China (Grant No. 52176034).

Conflict of Interest

The authors declare that they don’t have any conflict of interest.

Authors' contributions

Zhen Qu and Yong Li wrote the main manuscript text. Jintao Li, Kun Cai, Jun Long and Can Yao prepared all the figures. All authors reviewed the manuscript.

Availability of data and material

The data and material of this paper come from the experimental data of China aerospace engineering which are not publicly available.

Ethics approval

Not applicable.

Consent to participate

All authors participated in finishing the final manuscript.

Consent for publication

All authors approved the final manuscript and the submission to this journal.

References

1. Bearman P W, Downie M J, Graham J M R, et al. Forces on cylinders in viscous oscillatory flow at low Keulegan-Carpenter numbers. Journal of fluid mechanics, 1985, 154: 337–356.
2. Graham, E.W. and Rodriguez, A.M. Characteristics of Fuel Motion Which Affect Airplane Dynamics. Journal of Applied Mechanics, 1952, 19: 381–388.

3. Huang Huaide. Vibration engineering[M]. China Aerospace Publishing House, 1993.
4. Maleki A, Ziyaeifar M. Sloshing damping in cylindrical liquid storage tanks with baffles. Journal of Sound and Vibration, 2008, 311(1–2): 372–385.
5. Molin B, Remy F. Experimental and numerical study of the sloshing motion in a rectangular tank with a perforated screen. Journal of Fluids and Structures, 2013, 43: 463–480.
6. Moiseev N N. Introduction to the theory of oscillations of liquid-containing bodies. Advances in Applied Mechanics, 1964, 8: 233–289.
7. Moiseev N N, Petrov A A. The calculation of free oscillations of a liquid in a motionless container[J]. Advances in Applied Mechanics, 1966, 9: 91–154.
8. Mi-an Xue, Pengzhi Lin, Jinhai Zheng, et al. Effects of perforated baffle on reducing sloshing in rectangular tank: Experimental and numerical study. China Ocean Engineering Society and Springer-Verlag Berlin Heidelberg, 2013, 27(5): 615–628.
9. Nayak S K, Biswal K C. Nonlinear seismic response of a partially-filled rectangular liquid tank with a submerged block. Journal of Sound and Vibration, 2016, 368: 148–173.
10. Panigrahy P K, Saha U K, Maity D. Experimental studies on sloshing behavior due to horizontal movement of liquids in baffled tanks. Ocean engineering, 2009, 36(3–4): 213–222.
11. Qi Hu, Yong Li, Yao Can, et al. Experiment of Liquid Sloshing Performance in Bulky Propellant Tank. Aerospace Control and Application, 2016, 42(3): 44–48.
12. Shabana A A. Theory of vibration[M]. New York: Springer-Verlag, 1991.
13. Vergalla M D. Experimental and Numerical Framework for Characterization of Slosh Dynamics[D]. Florida Institute of Technology, USA, 2010.
14. Yan G, Rakheja S, Siddiqui K. Experimental study of liquid slosh dynamics in a partially-filled tank. Journal of fluids engineering, 2009, 131(7).

Figures

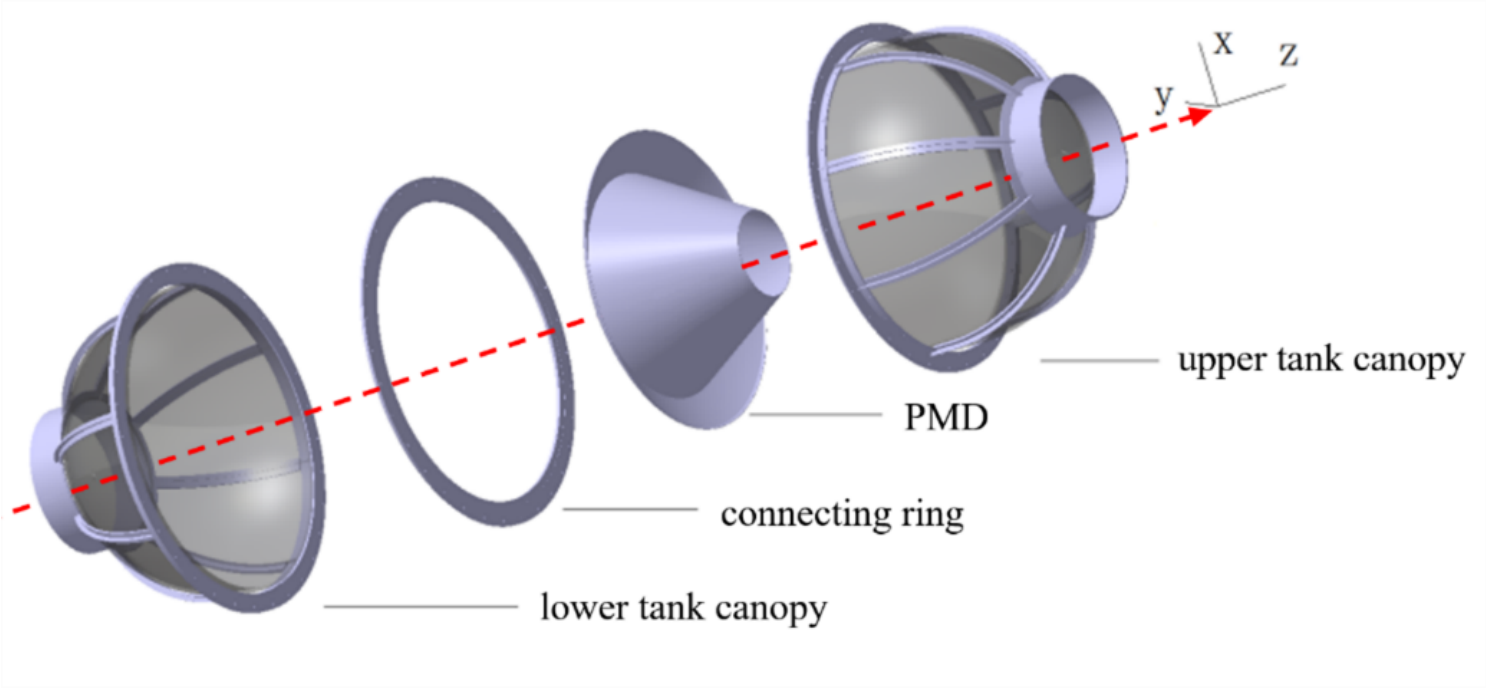

Figure 1

Test tank structure

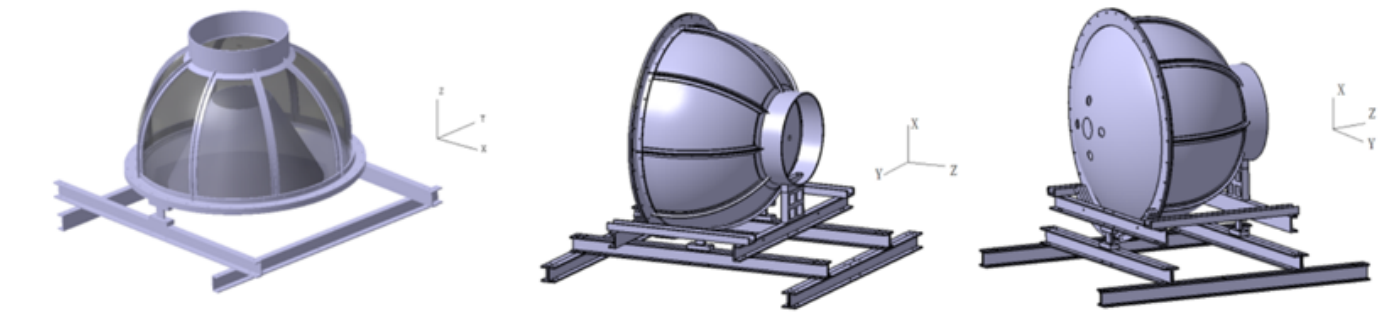

(a) ZX direction (b) XZ direction (c) XY direction

Figure 2

Three test directions of the upper tank with PMD.

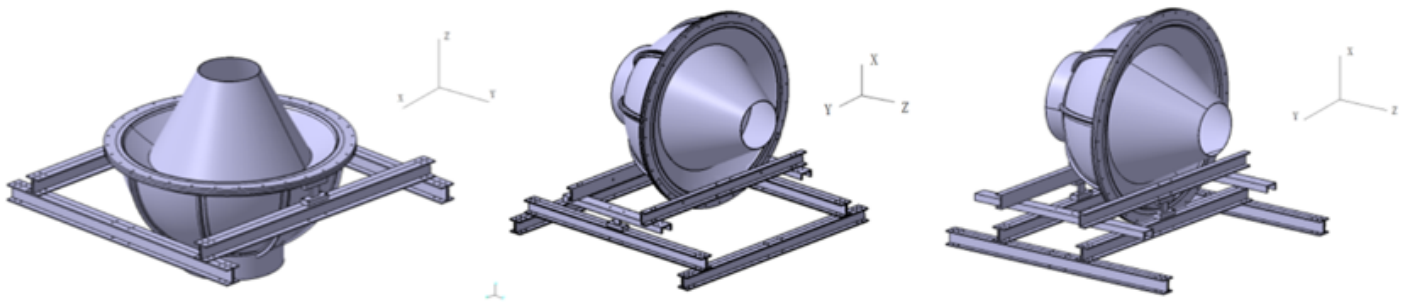

(a) ZX direction (b) XZ direction (c) XY direction

Figure 3

Three test directions of the lower tank.

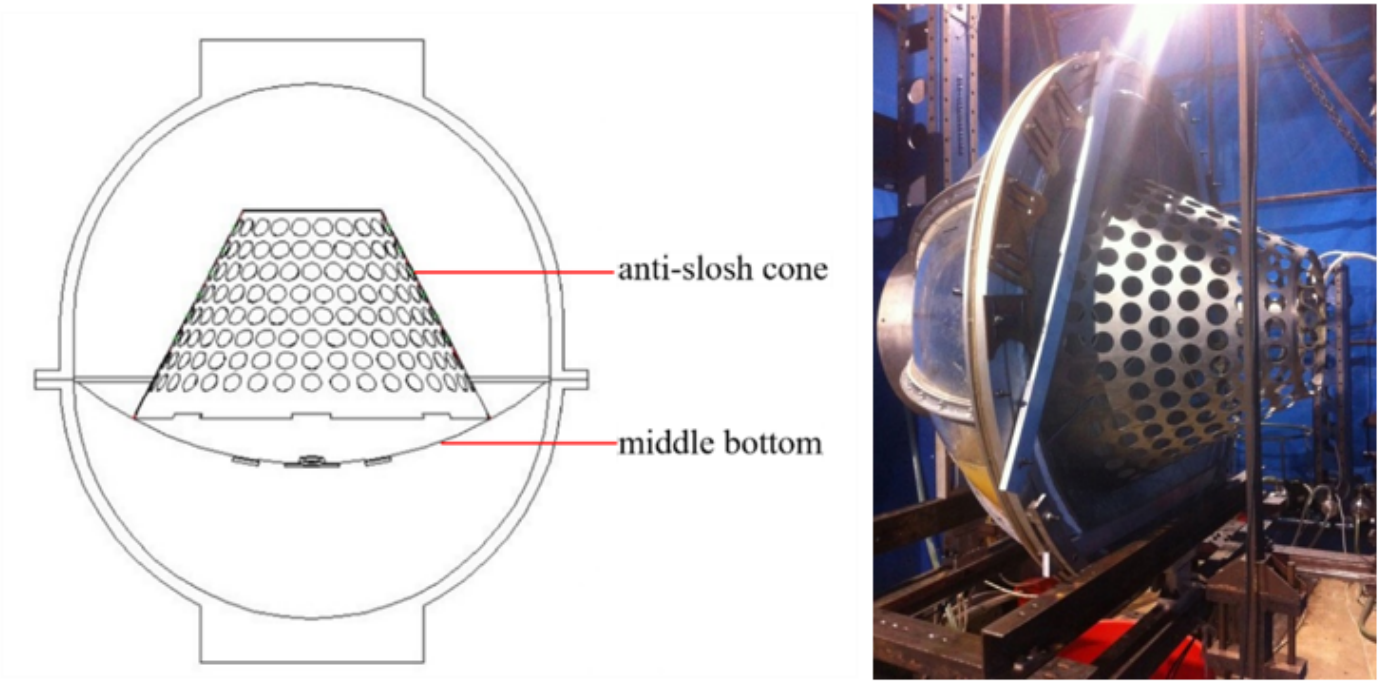

（a）Schematic （b）Tested structure

Figure 4

The structure of the anti-slosh cone and middle bottom.

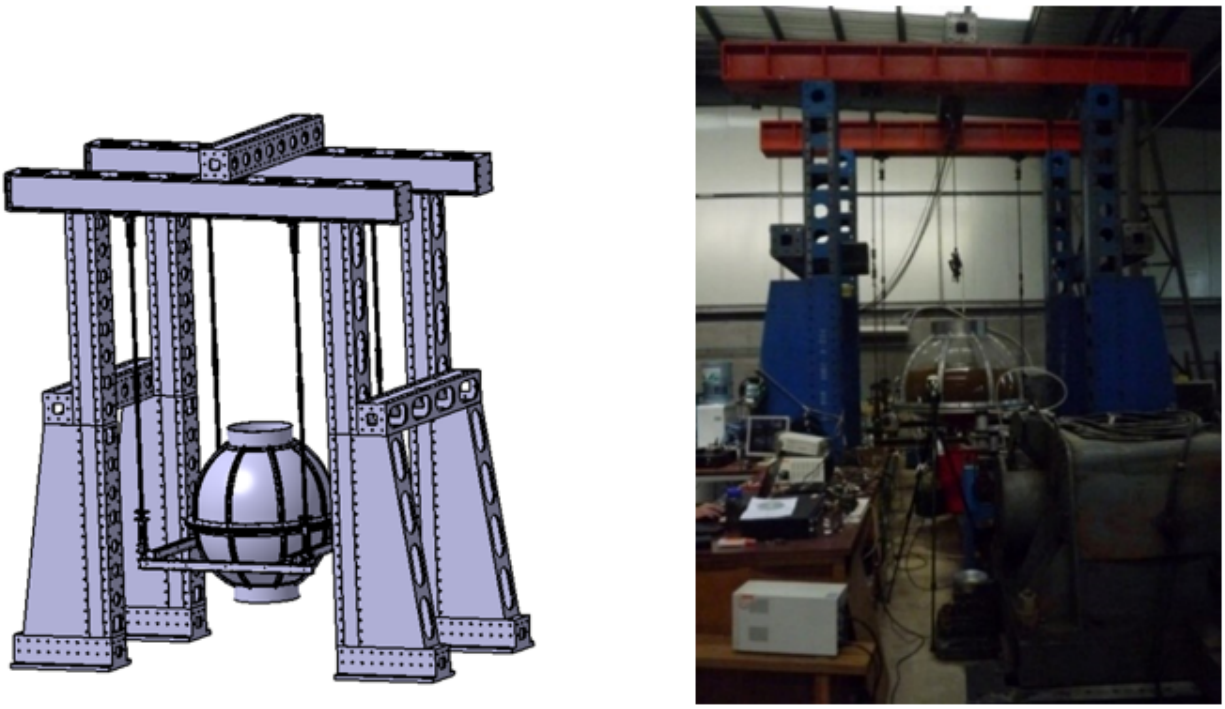

（a）schematic diagram　　（b）device diagram.

Figure 5

The liquid sloshing test device.

Figure 6

"Π" type force and torque sensors

Figure 7

Liquid sloshing test in the ZX direction of the upper tank.

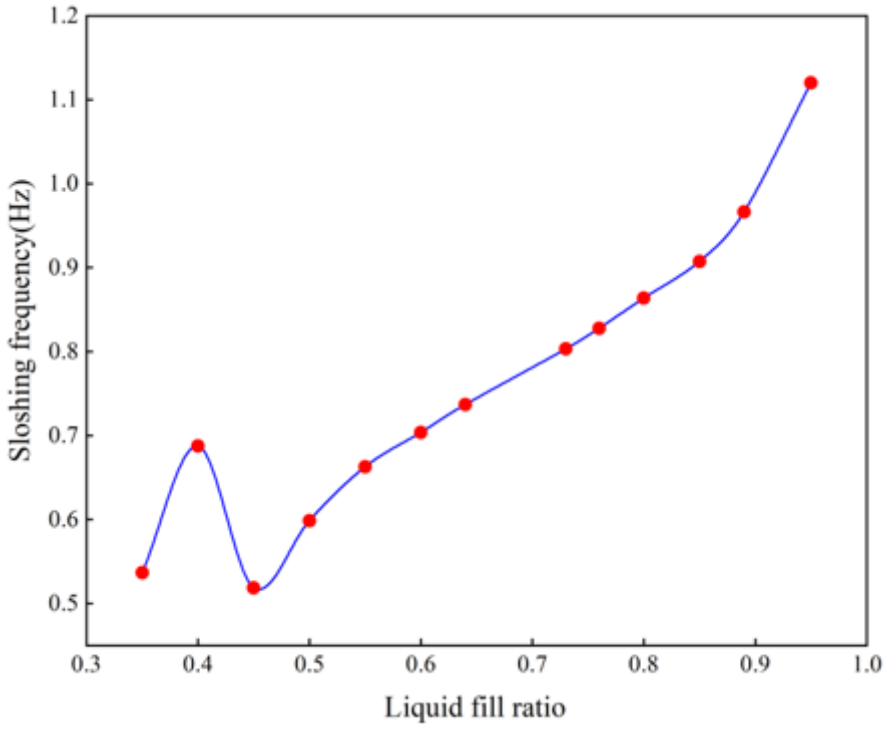

Figure 8

Tested sloshing frequency for the upper tank with PMD.

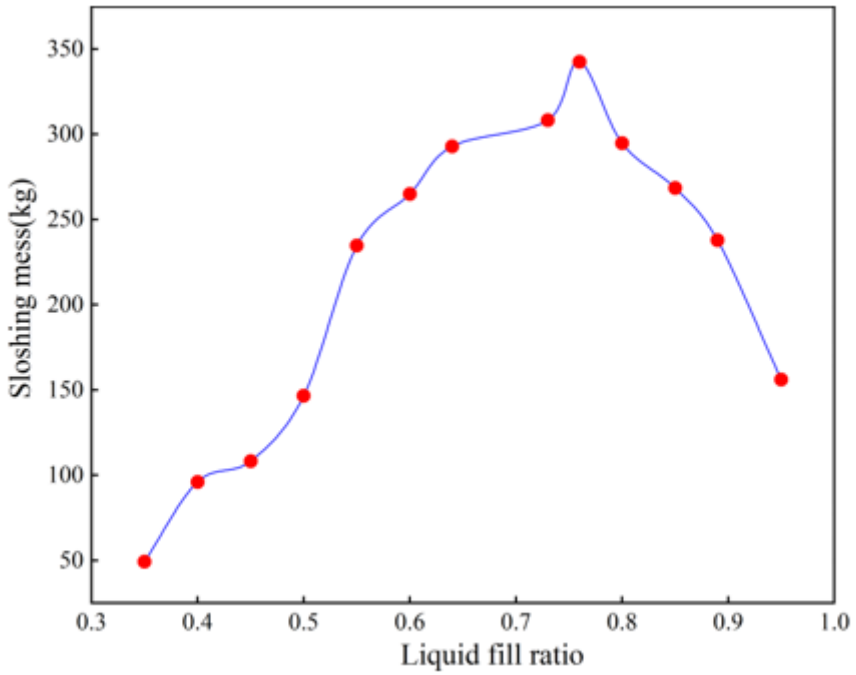

Figure 9

Test results of liquid sloshing quality in the upper tank with middle bottom.

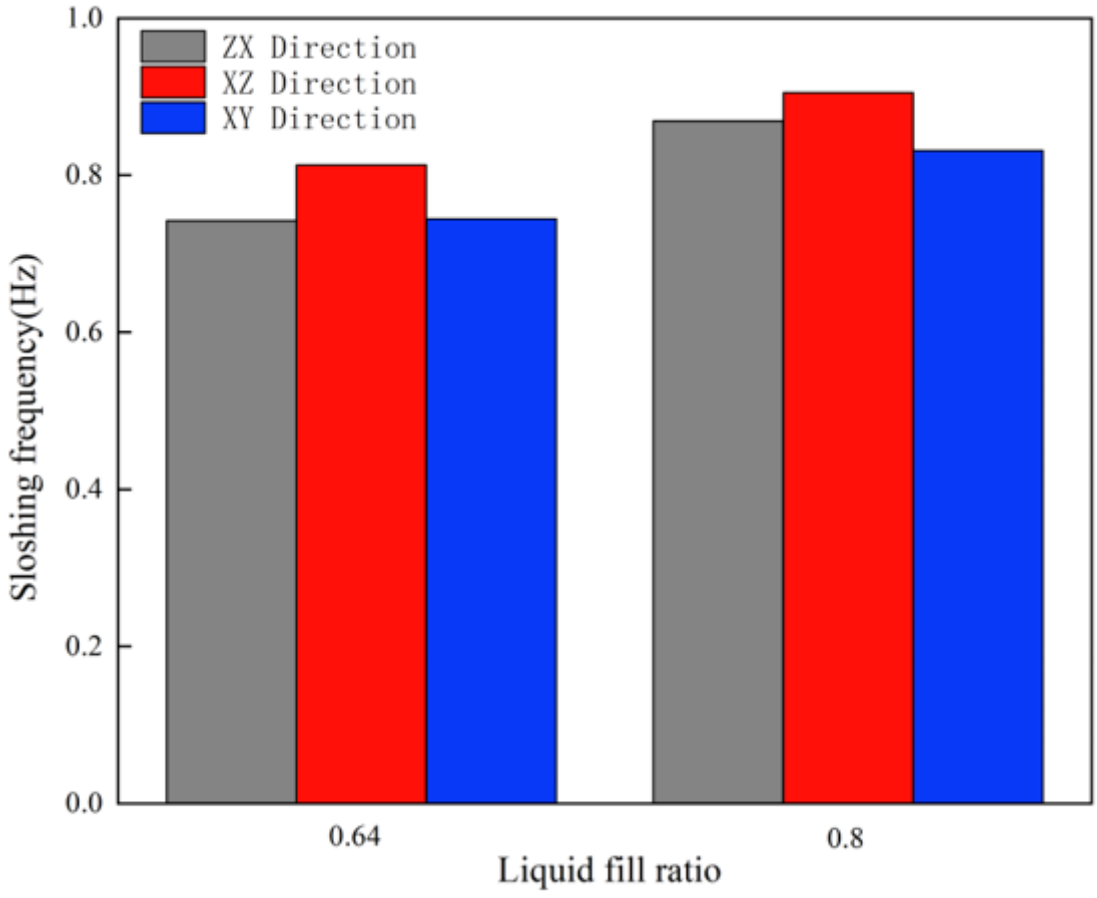

Figure 10

The frequency of liquid sloshing in the upper tank with the middle bottom (the filling ratio is constant at 0.64, 0.8).

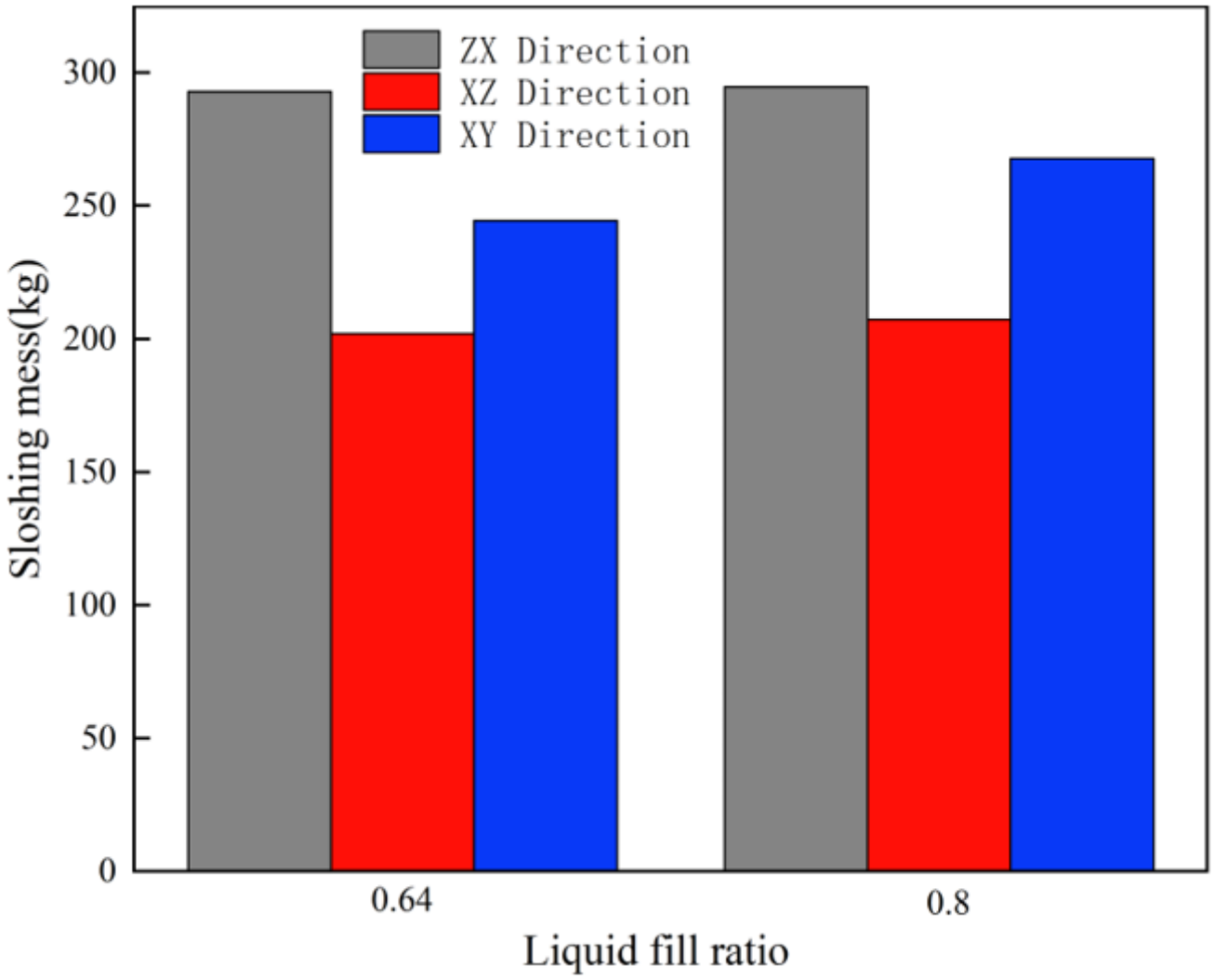

Figure 11

The sloshing mass of the liquid in the upper tank with the middle bottom (the filling ratio is constant at 0.64, 0.8).

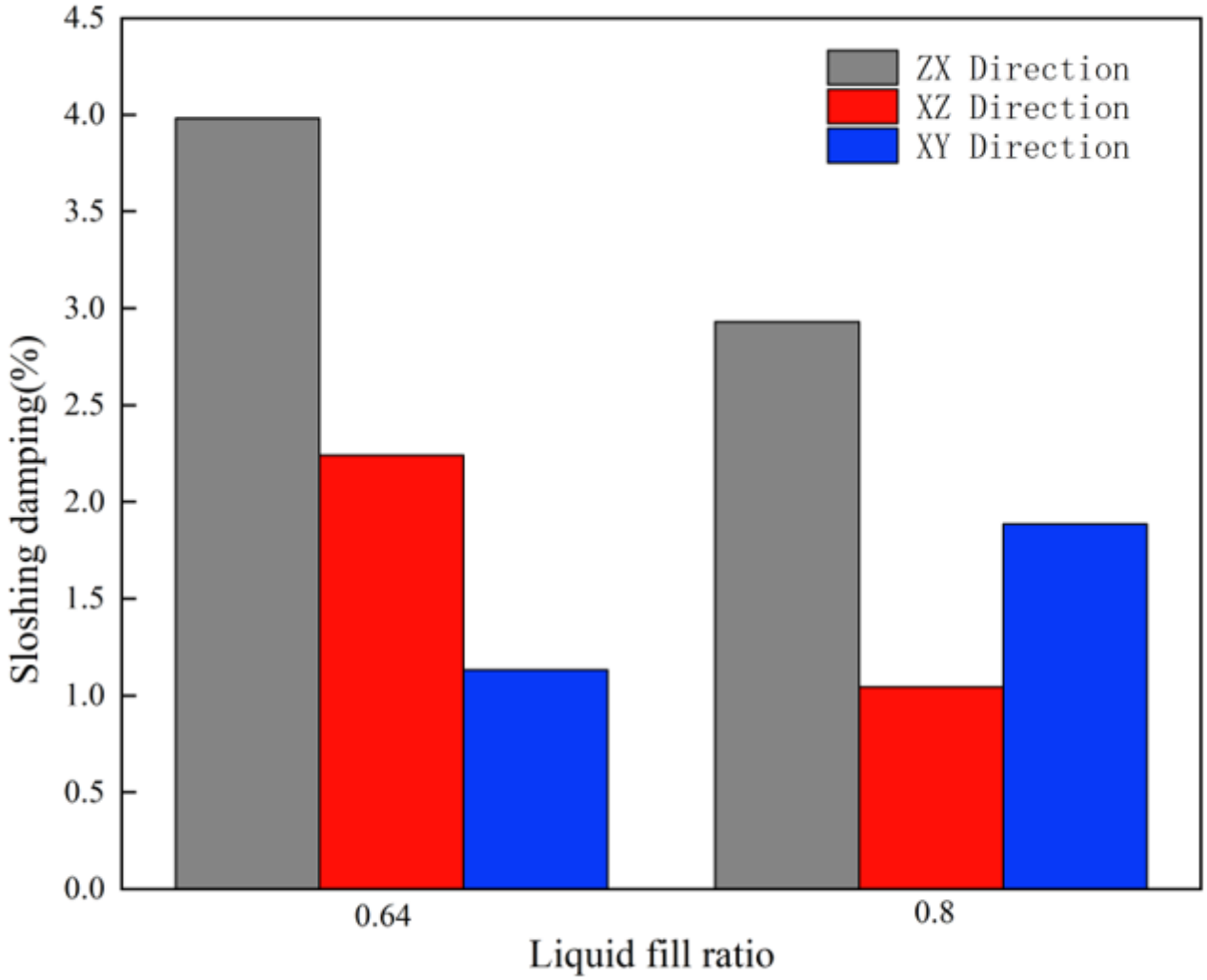

Figure 12

The sloshing damping of the liquid sloshing frequency of the upper tank with the middle bottom (the filling ratio is constant at 0.64, 0.8).

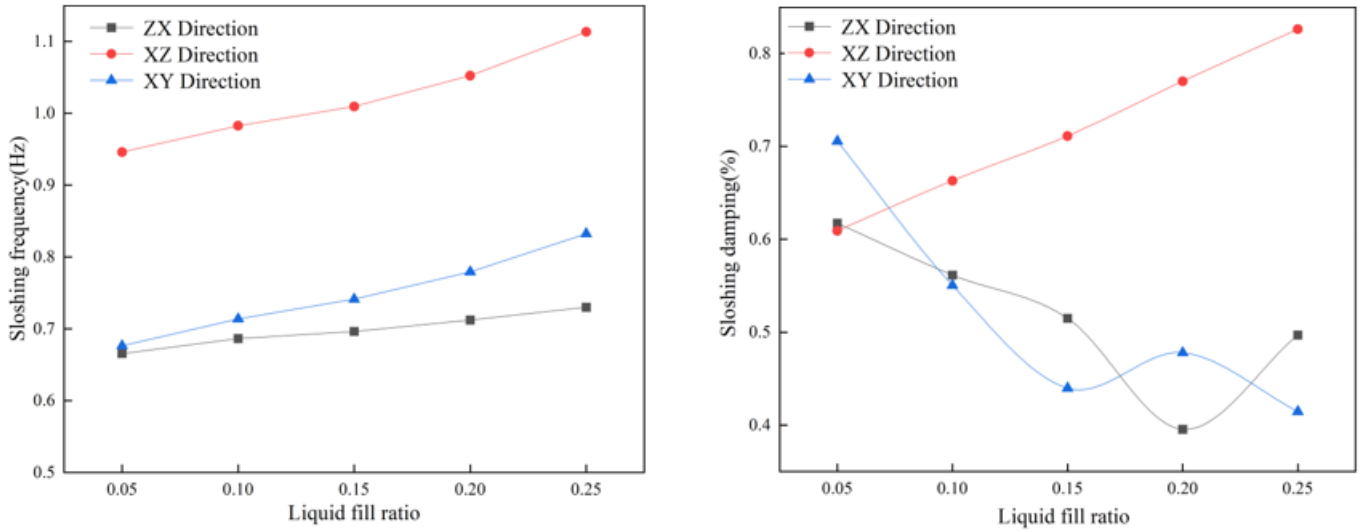

（a）sloshing frequency　　（b）sloshing damping

Figure 13

Experimental sloshing properties results of the lower tank.

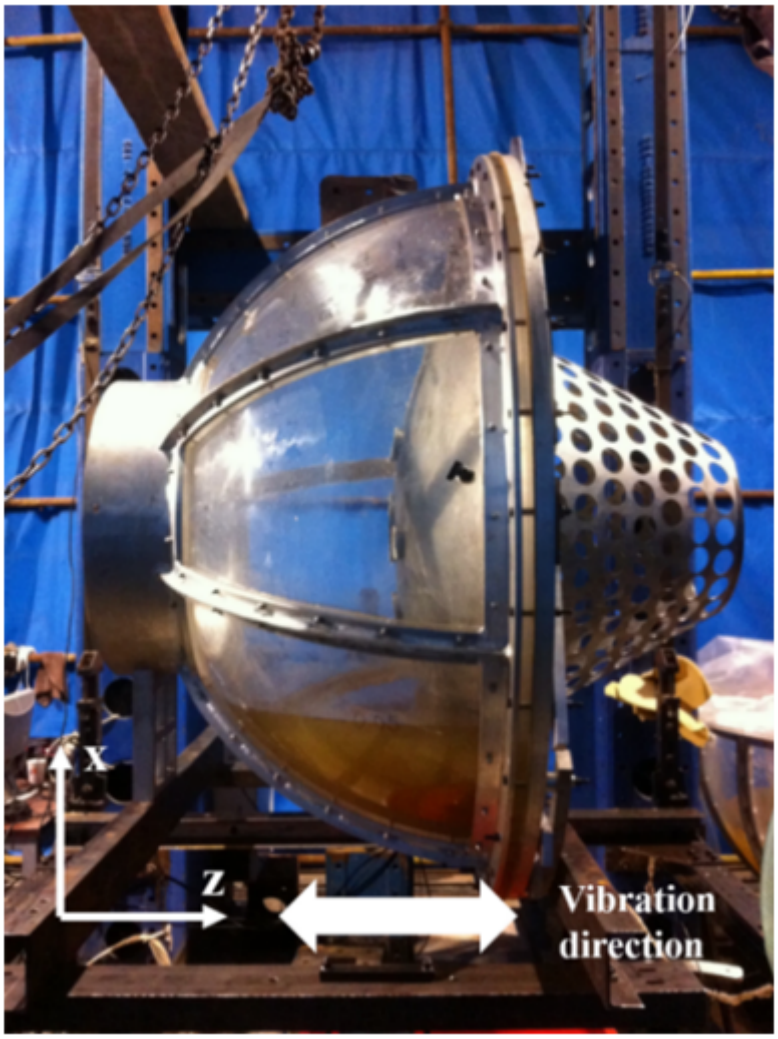

Figure 14

The experimental liquid sloshing in the XZ direction of the lower tank.

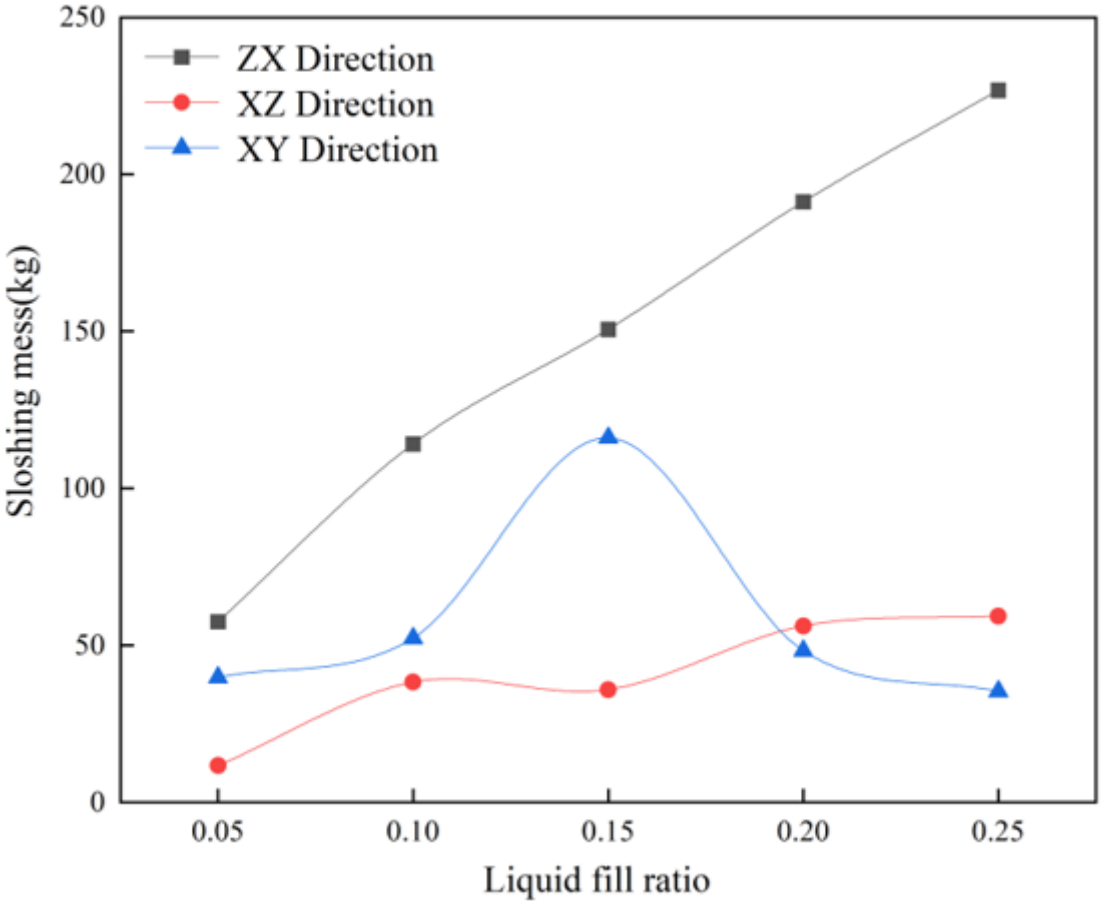

Figure 15

The sloshing mass of the liquid in the lower tank.

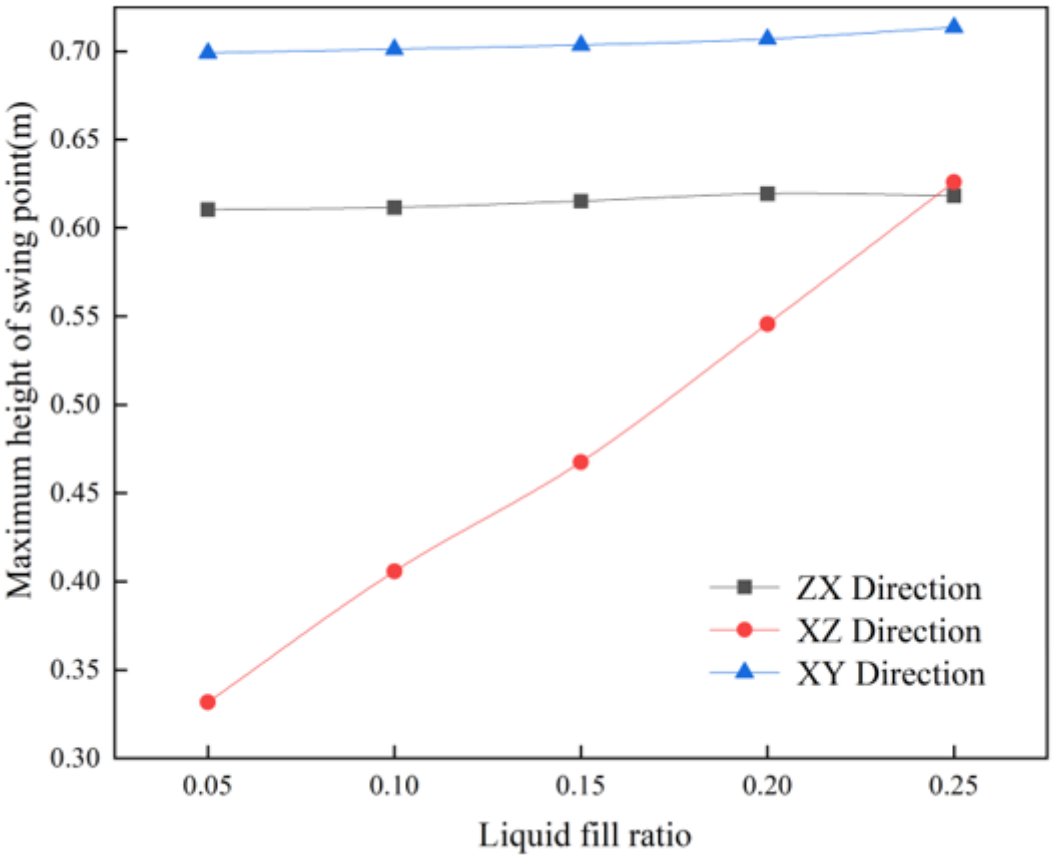

Figure 16

The maximum height of the swing point in the lower tank.